Layered Black Phosphorus as a Selective Vapor Sensor

Mayorga-Martinez, Carmen C.; Sofer, Zdeněk; Pumera, Martin

2015

https://hdl.handle.net/10356/83814

https://doi.org/10.1002/anie.201505015

Layered Black Phosphorus as a Selective Vapor Sensor

Carmen C. Mayorga-Martinez, Zdeněk Sofer, and Martin Pumera*

Abstract: Black phosphorus is a layered material that is sensitive to the surrounding atmosphere. This is generally considered as a disadvantage, especially when compared to more stable layered compounds, such as graphite or MoS_2. This sensitivity is now turned into an advantage. A vapor sensor that is based on layered black phosphorus and uses electrochemical impedance spectroscopy as the detection method is presented; the device selectively detects methanol vapor. The impedance phase measured at a constant frequency is used as a distinctive parameter for the selective quantification of methanol, and increases with the methanol concentration. The low detection limit of 28 ppm is well below the approved exposure limit of 200 ppm. The results are highly reproducible, and the vapor sensor is shown to be very selective in the presence of other vapors and to have long-term stability.

There is a high demand for sensitive and selective vapor sensors. The superior performance of graphene-based gas and vapor sensors[1] has led to the exploration of alternative two-dimensional materials for the development of such devices, such as transition-metal dichalcogenides (TMDs)[2] and the emerging class of 2D elemental materials, such as black phosphorus.[3] It was recently reported that few-layered black phosphorus displays anisotropic electrical conductance[4] and a direct band gap.[3a, 5] These attributes render it an excellent candidate for use in electronics and the development of electrochemical devices. Moreover, the electrical resistivity of black phosphorus is influenced by gas-molecule adsorption.[3a] Therefore, black phosphorus is a promising 2D material for gas/vapor-sensing applications. The detection of methanol is of very high importance because of its toxicity. Methanol is used industrially as a solvent, pesticide, and alternative fuel source. In industrial settings, the inhalation of high concentrations of methanol vapor and the absorption of methanol

through the skin are as effective as oral uptake in producing toxic effects. For these reasons, the National Institute for Occupational Safety and Health (NIOSH) of the US Centers for Disease Control and Prevention has set the occupational exposure limit for methanol vapor to 200 ppm.[6]

Electrochemical impedance spectroscopy (EIS) is a powerful technique that is used for surface characterization and as a transduction method in electrochemical biosensors.[7] Furthermore, this technique is effective in vapor detection.[1b,c, 9] An analytical signal characteristic of a specific analyte is crucial for the development of gas or vapor sensors. For this purpose, the consideration and application of new gas-sensitive materials and transduction are of great importance.[1a,b]

Herein, we report the development of a new device that is based on an interdigitated gold electrode modified with layered black phosphorus (Figure 1 A) for sensing methanol vapor using electrochemical impedance spectroscopy as the transduction method. We will show that such a device is highly sensitive and selective.

Layered black phosphorus was prepared by vapor transport growth from red phosphorus in the form of platelet crystals, as previously reported.[4a] The X-ray diffraction pattern of a sample of black phosphorus (Figure 1 B) shows highly preferential orientation along the (0k0) direction without any other phases. The black phosphorus has an orthorhombic crystal structure (space group *Cmce*), which is schematically shown in Figure 1 C. This effect originates from weak van der Waals bonds between individual phosphorus
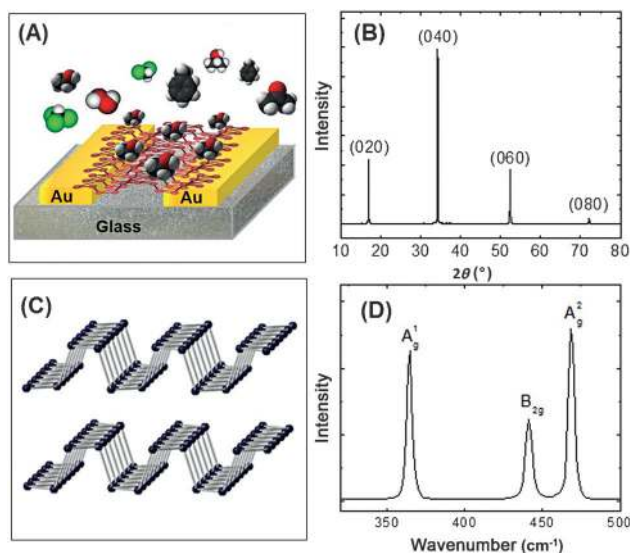
[*] Dr. C. C. Mayorga-Martinez, Prof. Dr. M. Pumera
    Division of Chemistry and Biological Chemistry
    School of Physical and Mathematical Sciences
    Nanyang Technological University
    Singapore 637371 (Singapore)
    E-mail: pumera.research@gmail.com

    Prof. Dr. Z. Sofer
    Department of Inorganic Chemistry
    University of Chemistry and Technology, Prague
    Technicka 5, 166 28 Prague 6 (Czech Republic)

Figure 1. a) Vapor sensor based on black phosphorus. B) X-ray diffractogram of black phosphorus. C) The crystalline structure of black phosphorus. D) Raman spectrum of black phosphorus.

layers. Raman spectroscopy gives three characteristic modes, A^1_g, B^2_g, and A^2_g, located at 364.6, 441.2, and 468.2 cm^{-1}, respectively. The Raman spectrum (Figure 1D) was obtained perpendicularly to the plane of the platelet crystals. The experimental data are in good agreement with values reported in the literature.[9]

Layered black phosphorus was deposited on an interdigitated gold electrode, and we monitored the changes in the electronic properties of the black phosphorus upon gas adsorption by impedance spectroscopy. We first focused on methanol vapors. Impedance Bode plots were recorded in a frequency range of 1 mHz to 100 kHz using a sinusoidal AC potential perturbation with a root mean square (RMS) of 0.01 V (Figure 2 and 3).
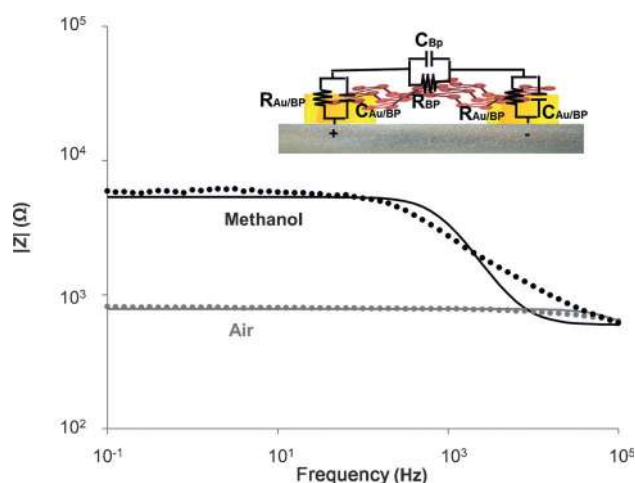

Figure 2. Experimental (•••••) and simulated (——) data for the impedance module of layered black phosphorus in the absence (air) and in the presence of 1140 ppm methanol vapor. Inset: Equivalent electrical circuit for modeling the impedance module data.

The impedance module increased in the presence of methanol vapors (black) with respect to the measurements conducted in air (gray) in all frequency ranges measured (see Figure 2). The experimental impedance module data (•••••) and the model data (——) that were obtained using a simplified equivalent circuit (Figure 2, inset) were also evaluated.

Considering the structure of the vapor sensor based on black phosphorus, the equivalent circuit includes three parallel resistor–capacitor (RC) circuits in series, the first and the last one corresponding to the interface between the gold electrode and the black phosphorus (BP) platelets ($C_{Au/BP}$ and $R_{Au/BP}$) whereas the second one corresponds to the interface between the black phosphorus platelets (C_{BP} and R_{BP}). Assuming that the first and third RCs correspond to the interface Au/BP, the total impedance could be expressed as Eq. (1). The resulting fitted data are given in Table 1.

$$|Z| = \frac{R_{Au/BP}}{1 + j\omega R_{Au/BP} C_{Au/BP}} + \frac{R_{BP}}{1 + j\omega R_{BP} C_{BP}} \qquad (1)$$

When the sensor is exposed to methanol, the capacitance of the Au/BP interface decreases by one order of magnitude

Table 1: Passive elements obtained from the equivalent electrical circuit proposed for modeling the impedance data of the black phosphorus based vapor sensor in air and in the presence of methanol vapor.

Passive elements	Air	Methanol
$R_{Au/BP}$ [Ω]	300	593
$C_{Au/BP}$ [nF]	5.71	0.207
R_{BP} [Ω]	480	4740
C_{BP} [nF]	63.3	42.6

while the resistance of the BP interface increases by a factor of ten.

The impedance phase spectra show a strong signal when recorded in the presence of methanol vapor at a resonance frequency of approximately 1 kHz (see Figure 3A). This peak
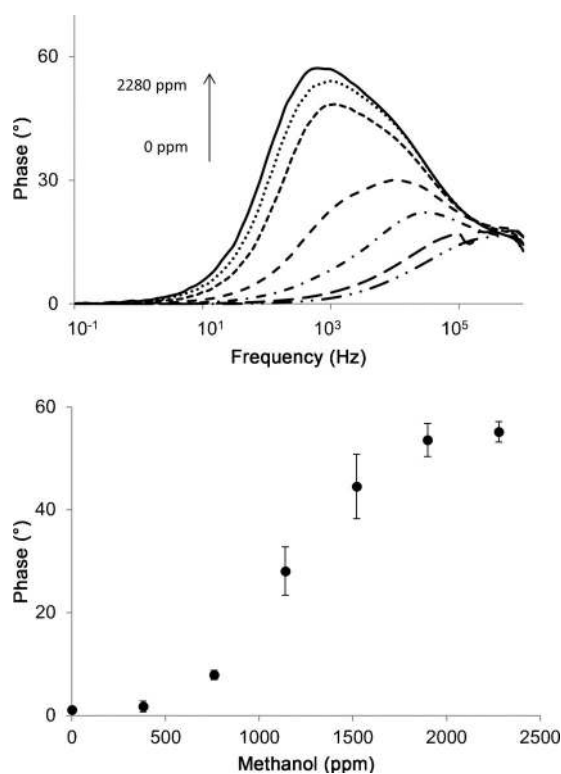

Figure 3. A) Impedance phase spectra of the black phosphorus device in the presence of different methanol vapor concentrations. B) Impedance phase at 1 kHz as a function of the methanol vapor concentration.

increases when the methanol concentration is increased. It is thus possible to utilize black phosphorus as a methanol vapor sensor. The impedance phase values recorded at a fixed frequency of 1 kHz as a function of methanol concentration are plotted in Figure 3B. The concentration dependence is linear in the range of 380–1900 ppm ($r = 0.9876$) before it levels off. Moreover, the sigmoidal profile of the calibration curve (Figure 3B) is in line with the general concentration response of sensors. These results confirm that the methanol molecules have a high affinity for the layered black phosphorus surface. With increasing methanol vapor concentration,

a rapid increase in the impedance response was observed until the saturation point, indicating a high sensitivity of the sensor towards methanol vapor.

Experiments with three different sensor devices showed good reproducibility and gave a relative standard deviation (RSD) of 18%. Even more importantly, this system is very sensitive with a low limit of detection (LOD) of 28 ppm. The LOD reported for this sensor is around seven times lower than the occupational exposure limit for methanol established by the NIOSH.[6]

The specificity of the vapor sensor based on black phosphorus was evaluated by recording the impedance phase after successive additions of toluene (2790 ppm), acetone (2535 ppm), chloroform (4775 ppm), dichloromethane (4262 ppm), ethanol (2519 ppm), isopropyl alcohol (2519 ppm), water (1602 ppm), and methanol (1140 ppm). The high specificity for methanol enables it to be distinguished from all the other vapors over the entire studied frequency range (see Figure 4 A), but methanol is most clearly detected at a frequency of 1 kHz (Figure 4 B).

Given that ethanol is the major contaminant of methanol, we examined how the presence of ethanol vapor influences the detection of methanol.[10] The impedance phase spectrum recorded in the presence of pure methanol is similar to that obtained in the presence of both methanol and ethanol vapors with a recovery of 83% (Supporting Information, Figure S1). We have thus confirmed the high selectivity of this system for methanol, which is due to the different dielectric constants of these molecules (MeOH: 32.7; EtOH: 24.6).[11] Thus, the impedance of black phosphorus differs upon the adsorption of methanol or ethanol vapors, thereby producing different responses. Within the accessible frequency range of 0.1 to 10 kHz, the impedance phase for methanol vapors could be most clearly measured at approximately 1 kHz. The resonance frequency of ethanol is $> 10^5$ Hz and thus enables the discrimination[12] of these compounds by electrochemical phase impedance measurements. For these reasons, this system shows a high selectivity for methanol vapor at a frequency of 1 kHz.

The long-term stability of the methanol vapor sensor based on black phosphorus was also studied (Figure 5). The impedance response of the sensor to 1140 ppm methanol was tested occasionally over a 20 day period. After the sensor had been exposed to methanol vapor, it was cleaned at 100°C for ten minutes. The average activity was found to be $90.13 \pm 9.27\%$ of the original response at the end of the 20 day period.
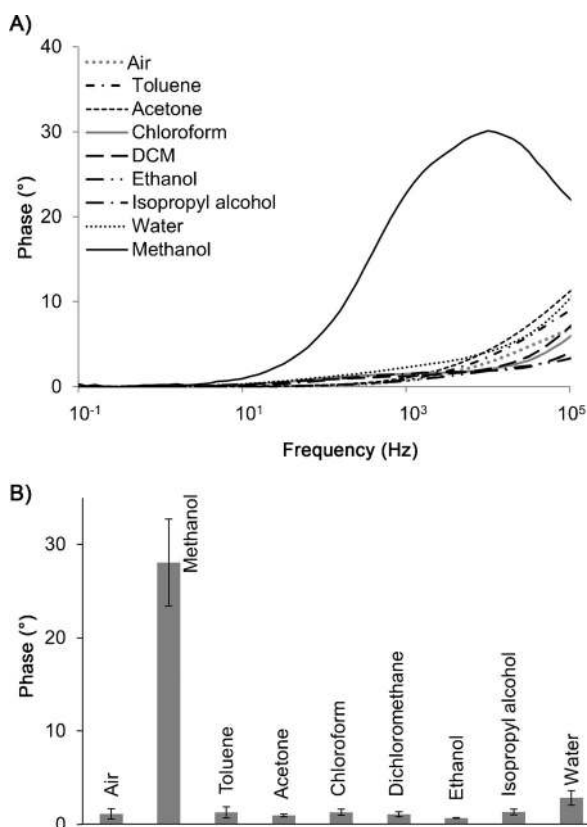

Figure 5. Long-term stability of the methanol vapor sensor based on black phosphorus.

In summary, we have developed a selective device for methanol sensing that is based on an interdigitated gold electrode modified with black phosphorus platelets. An equivalent circuit that describes the resistive and capacitive behaviors of the device has also been proposed. This device exhibits a distinctive peak in the impedance phase in the presence of different concentrations of methanol at resonance frequencies up to 1 kHz. The results were well reproducible, and the device displayed high sensitivity. The impedance phase depended linearly on the methanol concentration between 380 and 1900 ppm. The black phosphorus based device is a novel, robust, and cost-effective sensor for methanol detection and might find use in industrial settings as well as for safety applications, in particular for in-field use, as it does not require the processing of complex data. We have thus shown that the sensitivity of black phosphorus to the ambient conditions can be exploited for important applications. This finding paves the way for further studies on utilizing the sensitivity of layered elemental materials to their surroundings.

Figure 4. Selectivity study with the black phosphorus sensor. A) Impedance phase spectra and B) impedance phase at 1 kHz in the presence of either methanol (1140 ppm), toluene (2790 ppm), acetone (2535 ppm), chloroform (4775 ppm), dichloromethane (4262 ppm), ethanol (2519 ppm), isopropyl alcohol (2519 ppm), or water (1602 ppm). The concentrations of the interfering species are larger than that of the methanol vapor.
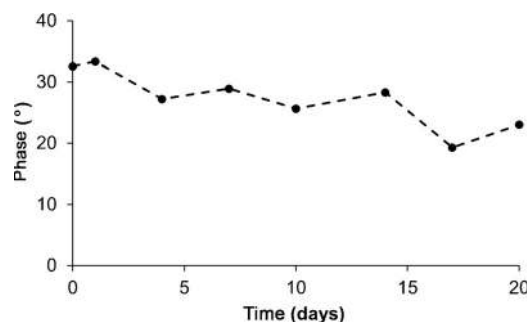
Experimental Section

The synthesis of black phosphorus crystals was based on a procedure reported in the literature[11] using a Au/Sn alloy-like solvent for red phosphorus (99.999% purity, Sigma–Aldrich, Czech Republic) and SnI_4 as a mineralizing agent in a sealed ampoule. 500 mg of the Au/Sn alloy were prepared by melting stoichiometric amounts of tin (99.999% purity, Sigma–Aldrich, Czech Republic) and gold (99.99% purity, Safina, Czech Republic) under high vacuum directly into the ampoule used for the synthesis. Red phosphorus (720 mg) and SnI_4 (15 mg) were added to a quartz ampoule and subsequently sealed by using an oxygen/hydrogen torch. The ampoule was placed in a muffle furnace and heated to 400°C for 1 h. After leaving it at 400°C for 2 h, the ampoule was heated to 600°C for 24 h. The furnace was then cooled to room temperature overnight. Crystals of black phosphorus in the shape of platelets of up to 5×2 mm were removed from the ampoule and washed with CS_2 to remove any white phosphorus formed as a side product. SnI_4 was prepared by direct synthesis using iodine (99.8%, PENTA, Czech Republic) and tin in chloroform (99.9%, PENTA, Czech Republic) under reflux. SnI_4 was purified by recrystallization from chloroform.

In a 312 mL glass chamber with a tightly closing lid, the liquid to be studied was placed in the desired atmosphere and allowed to stand for 30 min at room temperature for vapor saturation of the environment. Beforehand, an electrical connector for the interdigitated electrode had been installed in the chamber cover in a way that avoided any contact with the liquid. An interdigitated gold electrode (width: 10 μm, spacing: 5 μm; ALS Co., Japan) was modified with 1 μL of black phosphorus platelets dispersed in deionized water at a concentration of 1 mgmL^{-1}. The electrode was then dried under a lamp for 20 min, leaving a randomly deposited material film on the interdigitated area bridging the two Au electrode bands.

Impedance measurements were carried out at room temperature using an Autolab PGSTAT 204/FRA 32M potentiostat/galvanostat (Eco Chemie, Utrecht, The Netherlands) controlled by NOVA version 1.1 software (Eco Chemie). A sinusoidal potential modulation of ± 10 mV in amplitude in the 0.1 Hz to 100 kHz frequency range with a logarithmic scale of 10 points per decade was used. X-ray powder diffraction data were collected at room temperature with a Bruker D8 Discoverer powder diffractometer with Bragg–Brentano parafocusing geometry using Cu Kα radiation ($\lambda = 1.5418$ Å, $U = 40$ kV, $I = 30$ mA). The diffraction patterns were acquired with an ultrafast detector Lynxeye over an angular range of 10–80° (2θ) with a step size of 0.01678 (2θ). Data evaluation was performed using the EVA software package. An inVia Raman microscope (Renishaw, England) with a CCD detector was used for Raman spectroscopy in backscattering geometry. A Nd-YAG laser (532 nm, 50 mW) with a 50× magnification objective was used for the measurements. Instrument calibration was performed with a silicon reference, which gave a peak center at 520 cm^{-1} and a resolution of less than 1 cm^{-1}. To avoid radiation damage, the laser power output used for this measurement was kept at 5 mW.

Acknowledgements

[1] a) S. Rumyantsev, G. Liu, M. S. Shur, R. A. Potyrailo, A. A. Balandin, *Nano Lett.* **2012**, *12*, 2294–2298; b) A. Fattah, S. Khatami, C. C. Mayorga-Martinez, M. Medina-Sánchez, L. Baptista-Pires, A. Merkoçi, *Small* **2014**, *10*, 4193–4199; c) S. Borini, R. White, D. Wei, M. Astley, S. Haque, E. Spigone, N. Harris, J. Kivioja, T. Ryhänen, *ACS Nano* **2013**, *7*, 11166–11173.

[2] a) D. Sarkar, X. Xie, J. Kang, H. Zhang, W. Liu, J. Navarrete, M. Moskovits, K. Banerjee, *Nano Lett.* **2015**, *15*, 2852–2862; b) D. J. Late, Y. K. Huang, B. Liu, J. Acharya, S. N. Shirodkar, J. Luo, A. Yan, D. Charles, U. V. Waghmare, V. P. Dravid, C. N. R. Rao, *ACS Nano* **2013**, *7*, 4879–4891; c) M. O'Brien, K. Lee, R. Morrish, N. C. Berner, N. McEvoy, C. A. Woldend, G. S. Duesberg, *Chem. Phys. Lett.* **2014**, *615*, 6–10.

[3] a) L. Kou, T. Frauenheim, C. Chen, *J. Phys. Chem. Lett.* **2014**, *5*, 2675–2681; b) A. N. Abbas, B. Liu, L. Chen, Y. Ma, S. Cong, N. Aroonyadet, *ACS Nano* **2015**, *9*, 5618–5624.

[4] a) L. Wang, Z. Sofer, M. Pumera, *ChemElectroChem* **2015**, *2*, 324–327; b) R. Fei, L. Yang, *Nano Lett.* **2014**, *14*, 2884–2889; c) P. Yasaei, B. Kumar, T. Foroozan, C. Wang, M. Asadi, D. Tuschel, J. E. Indacochea, R. F. Klie, A. Salehi-Khojin, *Adv. Mater.* **2015**, *27*, 1887–1892; d) J. Qiao, X. Kong, Z.-X. Hu, F. Yang, W. Ji, *Nat. Commun.* **2014**, *5*, 4475.

[5] a) S. Balendhran, S. Walia, H. Nili, S. Sriram, M. Bhaskaran, *Small* **2015**, *11*, 640–652; b) Y. Du, H. Liu, Y. Deng, P. D. Ye, *ACS Nano* **2014**, *8*, 10035–10042; c) M. Buscema, D. J. Groenendijk, S. I. Blanter, G. A. Steele, H. S. J. van der Zant, A. Castellanos-Gomez, *Nano Lett.* **2014**, *14*, 3347–3352; d) L. Li, Y. Yu, G. J. Ye, Q. Ge, X. Ou, H. Wu, D. Feng, X. H. Chen, Y. Zhang, *Nat. Nanotechnol.* **2014**, *9*, 372–377; e) S. P. Koenig, R. A. Doganov, H. Schmidt, A. H. Castro Neto, B. Ozyilmaz, *Appl. Phys. Lett.* **2014**, *104*, 103106.

[6] The National Institute for Occupational Safety and Health (NIOSH), METHANOL: Systemic Agent; http://www.cdc.gov/niosh/ershdb/emergencyresponsecard_29750029.html, accessed: May **2015**.

[7] a) B.-Y. Chang, S.-M. Park, *Annu. Rev. Anal. Chem.* **2010**, *3*, 207–229; b) C. C. Mayorga Martinez, E. F. Treo, R. E. Madrid, C. C. Felice, *Biosens. Bioelectron.* **2010**, *26*, 1239–1244; c) C. C. Mayorga-Martinez, A. Chamorro-Garcia, A. Merkoçi, *Biosens. Bioelectron.* **2015**, *67*, 53–58.

[8] P. Karthick Kannan, R. Saraswathi, *Talanta* **2014**, *129*, 545–551.

[9] S. Sugai, I. Shirotani, *Solid State Commun.* **1985**, *53*, 753–755.

[10] S. Ishihara, N. Iyi, J. Labuta, K. Deguchi, S. Ohki, M. Tansho, T. Shimizu, Y. Yamauchi, P. Sahoo, M. Naito, H. Abe, J. P. Hill, K. Ariga, *ACS Appl. Mater. Interfaces* **2013**, *5*, 5927–5930.

[11] Common Organic Solvents: Table of Properties; https://www.organicdivision.org/orig/organic_solvents.html, accessed: August **2015**.

[12] C. C. Mayorga-Martinez, A. Ambrosi, A. Y. S. Eng, Z. Sofer, M. Pumera, *Adv. Funct. Mater.* **2015**, *25*, 5611–5616.